Washington University in St. Louis
SCHOOL OF MEDICINE

DEPARTMENT OF NEUROLOGY
NEUROMUSCULAR DIVISION
HOPE CENTER FOR NEUROLOGICAL DISORDERS

TIMOTHY M. MILLER, MD,PHD
660 S. EUCLID, CAMPUS BOX 8111
ST. LOUIS, MO 63110
PHONE: (314) 362-6981
FAX: (314) 362-3752
EMAIL: MILLER.T@WUSTL.EDU

I am pleased to provide you complimentary one-time access to my article as a PDF file for your own personal use. Any further/multiple distribution, publication or commercial usage of this copyrighted material would require submission of a permission request to the publisher.

Timothy M. Miller, MD, PhD
Professor of Neurology
Washington University School of Medicine

doi:10.1093/brain/awy182 BRAIN 2018: 141; 2561–2575 | 2561

BRAIN
A JOURNAL OF NEUROLOGY

Motor neuron-derived microRNAs cause astrocyte dysfunction in amyotrophic lateral sclerosis

Mariah L. Hoye,[1] Melissa R. Regan,[2] Leah A. Jensen,[1] Allison M. Lake,[3,4] Linga V. Reddy,[1] Svetlana Vidensky,[2] Jean-Philippe Richard,[2] Nicholas J. Maragakis,[2] Jeffrey D. Rothstein,[2] Joseph D. Dougherty[3,4] and Timothy M. Miller[1]

See Ferraiuolo and Shaw (doi:10.1093/brain/awy213) for a scientific commentary on this article.

We recently demonstrated that microRNA-218 (miR-218) is greatly enriched in motor neurons and is released extracellularly in amyotrophic lateral sclerosis model rats. To determine if the released, motor neuron-derived miR-218 may have a functional role in amyotrophic lateral sclerosis, we examined the effect of miR-218 on neighbouring astrocytes. Surprisingly, we found that extracellular, motor neuron-derived miR-218 can be taken up by astrocytes and is sufficient to downregulate an important glutamate transporter in astrocytes [excitatory amino acid transporter 2 (EAAT2)]. The effect of miR-218 on astrocytes extends beyond EAAT2 since miR-218 binding sites are enriched in mRNAs translationally downregulated in amyotrophic lateral sclerosis astrocytes. Inhibiting miR-218 with antisense oligonucleotides in amyotrophic lateral sclerosis model mice mitigates the loss of EAAT2 and other miR-218-mediated changes, providing an important *in vivo* demonstration of the relevance of microRNA-mediated communication between neurons and astrocytes. These data define a novel mechanism in neurodegeneration whereby microRNAs derived from dying neurons can directly modify the glial phenotype and cause astrocyte dysfunction.

1 Department of Neurology, Washington University School of Medicine; St. Louis, MO 63110, USA
2 Department of Neurology, Johns Hopkins University School of Medicine, Baltimore, MD 21205, USA
3 Department of Genetics, Washington University School of Medicine; St. Louis, MO 63110, USA
4 Department of Psychiatry, Washington University School of Medicine; St. Louis, MO 63110, USA

Correspondence to: Timothy Miller
Department of Neurology
Campus Box 8111; 660 S Euclid, St. Louis, MO 63110, USA
E-mail: miller.t@wustl.edu

Keywords: ALS; miR-218; extracellular miRNA; neuron-glia communication; non-cell autonomous

Abbreviations: ALS = amyotrophic lateral sclerosis; ASO = antisense oligonucleotide; EAAT2 = excitatory amino acid transporter 2

Introduction

Historically, neurodegeneration has been characterized by the pathological aggregates that accumulate in neurons and presumably lead to neuronal loss. However, over 10 years ago, seminal work in the field demonstrated that neurodegenerative diseases are partially non-cell autonomous, in that while neurons preferentially accumulate aggregates and degenerate, glial dysfunction most substantially contributes to ongoing neuronal loss and disease progression

Received January 07, 2018. Revised May 12, 2018. Accepted May 24, 2018. Advance Access publication July 10, 2018

(Boillee *et al.*, 2006; Yamanaka *et al.*, 2008*a*, *b*). Likewise, emerging genetic data suggesting glial-enriched genes are risk factors for neurodegenerative diseases have led to a resurgence in studying the glial contributions to disease progression (Guerreiro *et al.*, 2013; Jonsson *et al.*, 2013; Zhang *et al.*, 2013). The non-cell autonomous nature of neurodegenerative diseases has been best described in mouse models of amyotrophic lateral sclerosis (ALS), which is a highly progressive disease characterized by the loss of motor neurons in the brain and spinal cord. One key observation from these studies is that disease onset is autonomously driven by motor neuron injury, but the rate of progression is strongly influenced by glia. While glia normally function to support neurons, in ALS, these homeostatic roles are often lost (Van Damme *et al.*, 2007; Cassina *et al.*, 2008; Ferraiuolo *et al.*, 2011; Madji Hounoum *et al.*, 2017) and replaced with aberrant reactivity that can accelerate, rather than limit, neuronal damage (Butovsky *et al.*, 2014; Gallardo *et al.*, 2014; Endo *et al.*, 2015; Almad *et al.*, 2016; Liddelow *et al.*, 2017). Some of this glial reactivity is due to intrinsic factors; however, glial toxicity is most apparent after disease onset, which is driven by motor neuron loss. This indicates that neighbouring glia may respond to dying neurons and in turn, exacerbate their degeneration. However, the direct molecular underpinnings of this glial response to neuronal injury remain elusive.

In recent years, it has been shown that extracellular microRNAs (miRNAs) can mediate intercellular communication. MiRNAs are short, non-coding RNAs that regulate translation of target mRNAs. Most canonically, miRNAs repress mRNA translation by binding to the 3′ untranslated region (UTR) of target mRNAs (Ambros, 2004); however, some miRNAs can also promote translation. Because they bind to target mRNAs with only seven to nine nucleotides of complementarity, a single miRNA can regulate hundreds of targets and shape the translated expression profile of a cell (Lim *et al.*, 2005). More recently, it has been demonstrated that miRNAs can be released extracellularly either in vesicles or in complex with protein (Hunter *et al.*, 2008; Wang *et al.*, 2010; Arroyo *et al.*, 2011; Turchinovich *et al.*, 2011). We recently found that a motor neuron-specific miRNA, miR-218, is released extracellularly, subsequent to motor neuron loss, into the CSF of ALS model rats (Hoye *et al.*, 2017). In end-stage ALS rat CSF, the extracellular miR-218 levels are nearly 10-fold higher than pre-symptomatic rats. Previous work suggests that extracellular miRNAs can act as signalling molecules and mediate expression changes in recipient cells that have functional consequences (Valadi *et al.*, 2007; Mittelbrunn *et al.*, 2011; Lehmann *et al.*, 2012); however, the majority of these studies are in cell culture or involve the application of purified miRNA-containing vesicles to animals. We hypothesized that the increased CSF levels of motor neuron-derived miR-218 in ALS rodents would be sufficient to affect neighbouring glial cells *in vivo*. To test this, we identified putative glial targets of miR-218, including excitatory amino acid transporter 2 (EAAT2, encoded by *SLC1A2*), an astrocytic glutamate transporter. EAAT2 is an attractive candidate with which to study the potential role of extracellular, motor neuron-derived miR-218 on neighbouring astrocytes because it has already been demonstrated that EAAT2 is selectively and post-transcriptionally lost in both ALS patients and animal models (Rothstein *et al.*, 1995; Bristol and Rothstein, 1996; Howland *et al.*, 2002).

We tested the ability of astrocytes to take up extracellular, motor neuron-derived miR-218 and regulate astrocyte protein expression. Specifically, we confirmed that miR-218 can regulate EAAT2 by monitoring direct binding to the EAAT2 3′ UTR in cell culture and also by miR-218 overexpression in astrocytes. We extended our studies to animal models to determine whether blocking motor neuron-derived miR-218 prevented it from functionally regulating astrocyte expression. We thus demonstrate a link between motor neuron-derived miRNAs and astrocyte dysfunction. This establishes a novel cellular pathogenic mechanism in neurodegeneration.

Materials and methods

Luciferase assays

Fragments of the EAAT2 3′ UTR containing miR-218 binding were generated via PCR using mouse BAC RPCI-23-361H22 (BACPAC Resources, bacpac.chori.org) and cloned into the PGL3-Control Vector (Promega, E1741). The eight regions and the primers used to generate them are shown in Supplementary Table 1. HEK293 cells were seeded 20 000 per well in 96-well plates the day prior to transfection. The next day, the cells were transfected with 0.15 µg luciferase reporter construct, 18–66 nM miR-218 (Dharmacon), and 0.015 µg *Renilla* luciferase vector pRL-TK (Promega, pRL-TK, E2241) for normalization. All transfections were carried out with Lipofectamine® 2000 (Invitrogen) according to the manufacturer's instructions. Luciferase activity was measured 48 h after transfection using the Dual-Glo® Luciferase kit (Promega E2920). Triplicates for each combination of reagents were assayed on a plate and averaged. Each set of conditions was repeated on two to nine plates. The results from each plate were averaged to assess the relative binding strength of each region.

Primary astrocyte culture

Mouse astrocyte cultures were made from the cortices of C57wt/BL6 postnatal Day 2 (P2) pups and maintained in Dulbecco's modified Eagle medium with 10% foetal bovine serum and incubated at 5% CO_2 and 37°C. Astrocytes were seeded at 100 000 cells per well in 6-well plates. The following day, they were transfected with 1.6 µg of scrambled miRNA or miR-218. In Fig. 4C, media from sporadic ALS induced pluripotent stem cell (iPSC)-derived motor neurons (line JH046; obtained at 55–65 days post-induction and cultured as described previously in Hoye *et al.*, 2017) or neuronal media not cultured with iPSC-derived motor neurons was diluted 10× in astrocyte media with or without 1 µM anti-miR-218 antisense oligonucleotides (ASOs). Of note, the sporadic ALS iPSC-derived motor neurons did not have an observable

degeneration phenotype. Seventy-two hours later, protein was isolated from the astrocytes in RIPA buffer (Cell Signaling Technologies, 9806).

Immunoblotting

Protein lysates were sonicated and spun at 10 000 *g* to pellet cellular debris. Protein concentration was determined using a BCA assay (Pierce) and then 10 µg of protein was diluted 1:1 in sample buffer (Bio-Rad, 1610737). Samples were denatured at 95°C for 10 min prior to loading on a 4–20% polyacrylamide gel (Bio-Rad) with precision plus protein ladder (Bio-Rad, 1610374). Non-specific sites were blocked in 5% milk and incubated overnight at 4°C with rabbit anti-GAPDH (Cell Signaling Technology, 14C10; 1:2500) and rabbit anti-EAAT2 (Abcam, ab41621; 1:1000), rabbit anti-Cx43 (Abcam, ab11370; 1:5000), rabbit anti-GFAP (Dako, Z0334; 1:500), or rabbit anti-EAAT1 (Abcam, ab416; 1:1000). Antibody labelling was detected by incubating blots with horseradish peroxidase-labelled anti-rabbit secondary antibody (GE Healthcare, NA934; 1:5000) and visualized using enhanced chemiluminescence (Pierce, 32106).

Animals

All animal protocols were approved by the Institutional Animal Care and Use Committee of Washington University at St. Louis and adhered to NIH and ARRIVE guidelines. All mice were bred on a congenic C57BL/6 J background, including the ALS model mice: C57Bl/6 J SOD1^{G93A} mice (ID: 004435). To generate cell-specific GFP-myc-Ago2 expressing mice, a homozygous (ROSA)26Sortm1(CAG-GFP/EiF2c2)Zjh (LSL-tAgo2) mouse (RRID:IMSR_JAX:017626) was bred to GFAP-Cre (Bajenaru *et al.*, 2002) (a gift from David H. Gutmann) and further crossed to C57Bl/6 J SOD1^{G93A} mice.

Experimental design

Both male and female mice were used for all experiments and sexes were equally distributed among groups. Littermates were used for all experiments and were randomly assigned to groups. Blinding was performed by concealing the treatment group during all downstream analyses.

Immunofluorescence

Free-floating 40 µm sections from 4% paraformaldehyde (PFA) fixed spinal cord tissue were used for immunofluorescence. Rabbit anti-EAAT2 (Abcam, ab41621; 1:1000), rabbit anti-Cx43 (Abcam, ab11370; 1:2000), or chicken anti-GFAP (Millipore, AB5541; 1:1000) was applied to the tissues overnight at 4°C. Secondary antibodies were applied to the tissue for 1 h. All sections were stained with DAPI. Slides were mounted and coverslipped with Fluoromount^{TM} (Southern Biotech, 0100-01). Images were acquired with a Nikon A1Rsi Confocal at ×20 magnification. For formatting, ImageJ and Adobe Photoshop CS6 Extended were used.

In situ hybridization

In situ hybridization was performed as described previously (Hoye *et al.*, 2017).

MiRNA tagging and affinity purification

Spinal cords from Day 70 (pre-symptomatic) and Day 140 (end-stage), saline perfused, LSL-tAgo2, GFAP Cre, SOD1^{G93A} or LSL-tAgo2, GFAP Cre only mice were harvested, flash frozen in liquid nitrogen, and stored at −80°C. MiRNA tagging and affinity purification (miRAP) was conducted as described previously (Hoye *et al.*, 2017).

RNA extraction and quantification

RNA was isolated using miRNeasy® kits per manufacturer's instructions (Qiagen). miRNA targets were assayed with individual TaqMan® miRNA qPCR assays (Life Technologies) in technical duplicates on an Applied Biosystems 7500 fast Real-Time PCR System.

MiR-218 uptake reporter assays

Four repeats of 100% complementary miR-218-5p sites were generated from IDT and cloned into the RNAi-Inducible Luciferase Expression System (RILES) vector. To make the system Cre inducible, primers containing flanking loxP sites were used to amplify inverted firefly luciferase (Fluc). This inverted Fluc, flanked by loxP sites, was then cloned into the RILES vector using SalI via In-Fusion cloning (as per manufacturer's instructions).

Primary astrocytes were seeded at 15 000 cells per well of a 96-well plate. The following day, 125 ng of the RILES vector, containing either miR-218 sites or siRNA to GFP sites, and 75 ng of CMV-Cre or empty vector control were transfected into astrocytes using Lipofectamine^{TM} 2000 (according to the manufacturer's instructions). Six hours later, the media was changed. To model extracellular miR-218, media from lysed NSC-34 cells (CELLutions) was obtained through three freeze-thaw cycles, centrifuged at 1000*g* for 5 min to pellet cellular debris, and filtered through a 0.22 µm filter. This media was then applied to astrocytes the day after transfection. Media from lysed NSC-34 cells (Cashman *et al.*, 1992) was added to astrocytes such that extracellular miR-218 was ∼10-fold higher. In Fig. 4D, media from sporadic ALS iPSC-derived motor neurons (line JH036) or neuronal media not cultured with iPSC-derived motor neurons was diluted 1 × in astrocyte media with or without 1 µM anti-miR-218 ASO and applied to primary astrocytes the day after transfection. Seventy-two hours post-transfection, Fluc was measured using the Dual-Glo® Luciferase kit (Promega, E2920) as described above.

Extracellular miR-218 assays

End-stage SOD1^{G93A} rat CSF was harvested as previously described (Hoye *et al.*, 2017). CSF was aliquoted into four different fractions: no treatment; RNase A treatment; RNase A and proteinase K treatment; or RNase A proteinase K and Triton^{TM} X-100 treatment. For RNase A treatment, 1 µg/ml of

RNase A (Thermo; R1253) was added and the sample was incubated for 15 min at 37°C. For RNase A and proteinase K treatment, the sample was preincubated with 5 µg/µl proteinase K (NEB; P8107S) for 30 min at 55°C before RNase A treatment. For RNase A, proteinase K and Triton™ X-100 treatment, the samples were pre-incubated with 1.5% Triton™ X-100 (final: 0.75%) before addition of proteinase K and RNase A.

Precipitation of miR-218 using biotinylated oligonucleotides

End-stage SOD1^{G93A} rat CSF was used to precipitate miR-218. Biotinylated anti-miR-218 oligonucleotides were purchased from IDT. Biotinylated oligonucleotides (10 µM) were conjugated to 30 µl of MyOne Streptavidin C1 beads (Invitrogen; 650-01) for 30 min at 4°C. The beads were washed thoroughly with buffer (10 mM KCl, 1.5 mM $MgCl_2$, 1 M NaCl, 10 mM Tris-HCl pH 7.5, 5 mM DTT, 0.5% Sigma-IGEPAL, 60 U/ml SUPERase In™) (Ambion; AM2694) and 1× complete mini protease inhibitor (Roche; 11836170001) before applying 300 µl of CSF with end-over rotating for 30 min at 4°C. The beads were thoroughly washed and QIAzol® was added directly to the beads.

Intracerebroventricular injections

For a detailed visual protocol, see DeVos and Miller (2013*b*). Prior to surgery, mice received 2–3% inhalant isoflurane for anaesthetization. The hair on the scalp was shaved and the mouse was placed in a stereotaxic head frame (Kopf). While under continued 2.5% isoflurane flow, a scalp incision was made and bregma was identified using hydrogen peroxide. The stereotactic injector was positioned −1 mm M/L, −0.3 mm A/P, −3 mm D/V from bregma. At 110 days of age, two cohorts of three to four C57Bl/6 J SOD1^{G93A} mice/group were injected with 10 µl of saline (Hospira; NDC 0409-4888-02) or anti-miR-218 ASO (10 µg/µl; IDT; 2′ *O*-methyl RNA bases, phosphorothioate bonds 5′-ACUGGUUAGAUCA AGCACAA-3′) into the intraventricular space. The incision was closed and mice were placed on a 37°C warming recovery pad until ambulatory. Mice were monitored once per day for 2 days following surgery. Downstream analyses were conducted by a blinded reviewer.

Polysome profiling

Sucrose gradients made with DEPC water (7%, 17%, 47% sucrose in 10 mM Tris pH 7.4, 60 mM KCl, 10 mM $MgCl_2$, 1 mM DTT) were poured in 12 ml Beckman ultracentrifuge tubes and equilibrated overnight at 4°C. The next day, whole brainstem was homogenized in polysome lysis buffer [10 mM Tris HCl pH 7.4, 130 mM KCl, 10 mM $MgCl_2$, 0.5 mM DTT, 0.5% NP-40, 100 µg/ml cycloheximide (Sigma, C7698) and 100 U/ml RNase inhibitor (Promega, N2615)]. The lysate was incubated on ice for 20 min and then spun at 13 000*g* for 10 min at 4°C. 350 µl of cleared lysate was applied to the top of the sucrose gradient and centrifuged at 200 000*g* (SW41Ti rotor) for 3 h at 4°C. Polysomes were fractionated into twenty-three 500-µl fractions using an Isco fractionation system. Polysome-containing fractions were determined based on the UV absorbance. QIAzol® was added directly to the fraction and miRNA was isolated using the miRNeasy® kit (Qiagen, 217004).

Quantification of fluorescence

Images were acquired with a Nikon A1Rsi Confocal at ×20 magnification with the same laser power and pinhole size, with the detector set so that no saturation occurred. The anterior horn of each spinal cord section was outlined and the mean fluorescence intensity was quantified using ImageJ. Image analyses were conducted by a blinded reviewer. Subsequent to quantification, images were equivalently brightened where denoted in the figure legend.

Statistical analysis

Data are presented as mean ± standard error of the mean (SEM). All statistical tests were conducted using R's Bioconductor toolkit, MS Excel or Graphpad Prism 6 Software. Because the data in Figs 5, 6 and 7 were all generated from the same cohort of mice, these data were corrected for multiple comparisons using the Benjamini-Hochberg correction (Klipper-Aurbach *et al.*, 1995) and a false discovery rate (FDR) of 0.1. To determine statistical significance of the overlap between translated mRNAs in ALS astrocytes and miRNA targets, we performed a Fisher's exact test, using all of the putative miR-218, miR-431, and miR-382 targets and 23 000 genes for the mouse genome and correcting for multiple (three) comparisons (Bonferroni). The statistical details for individual experiments can be found in the corresponding figure legends.

Data availability

The data that support the findings of this study are available from the corresponding author, upon reasonable request.

Results

Prediction of putative glial targets of miR-218

To determine whether extracellular, motor neuron-derived miR-218 could be taken up by neighbouring glia in ALS and exert functional consequences, we sought to identify putative glial targets of miR-218. To this end, we used RNA sequence data generated by Zhang and colleagues (2014) from different purified CNS cell types. We identified the top transcripts that were enriched in microglia, astrocytes or oligodendrocytes and determined whether any were putative miR-218 targets (Supplementary Table 2). Among the top glial targets of miR-218, we identified EAAT2 (also known as GLT-1 in rodents, gene *Slc1a2*) as an attractive candidate. EAAT2 is a glutamate reuptake transporter specifically enriched in healthy astrocytes; however, its loss has already been well-established in both ALS patients and animal models (Rothstein *et al.*, 1995; Howland *et al.*, 2002). Furthermore, this loss of EAAT2

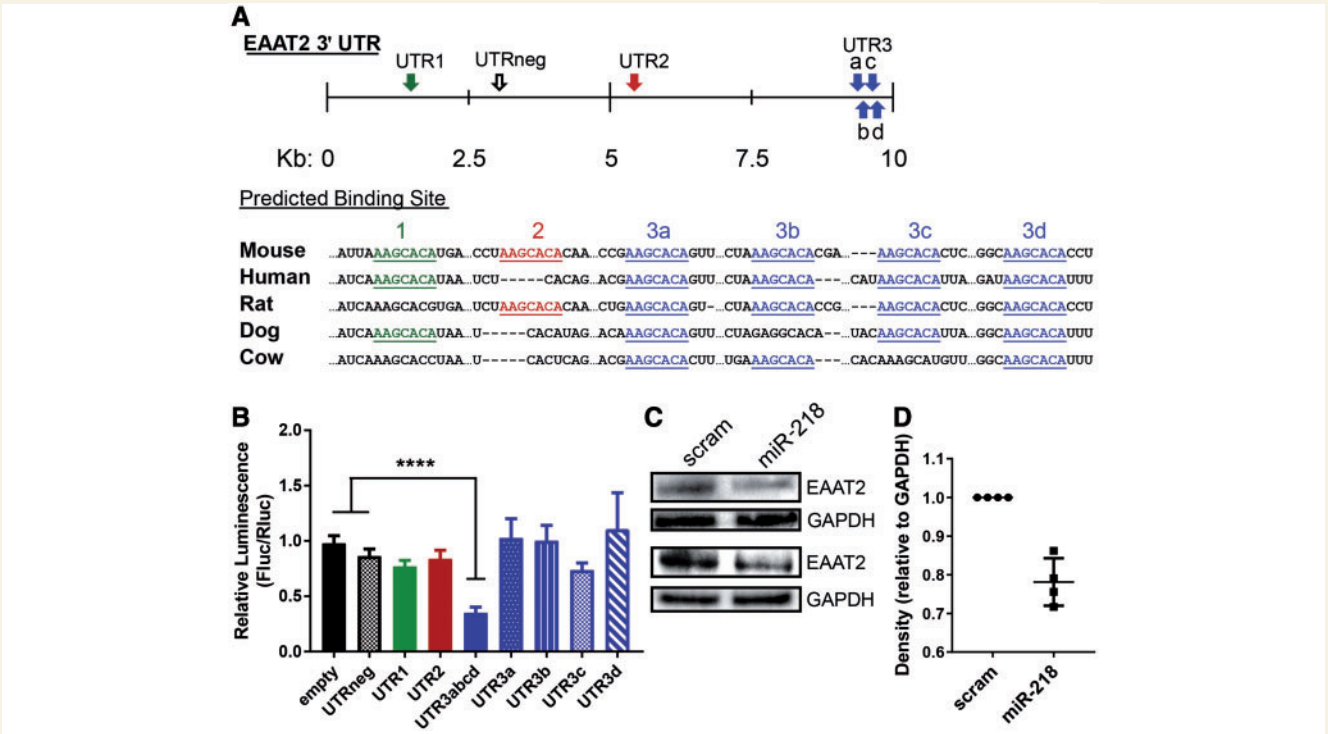

Figure 1 MiR-218 directly regulates EAAT2 expression through 3′ UTR binding and is sufficient for EAAT2 loss. (**A**) Schematic of the mouse EAAT2 3′ UTR indicating six putative miR-218 binding sites (targetscan.org) and the sequence conservation in select mammals. (**B**) Luciferase assays were performed to assess the relative strength of miR-218 binding sites in the EAAT2 3′ UTR as compared to empty vector and negative control *Slc1a2*/EAAT2 3′ UTR. $n = 3$ replicates/trial and 2–9 trials/condition. (**C**) Transient transfection of primary astrocytes with miR-218, but not scrambled miRNA results in EAAT2 loss. $n = 4$. The monomer EAAT2 band (~60 kDa) is shown. (**D**) Quantification of westerns from four independent trials of **C**. Density is represented relative to GAPDH for the corresponding trial. Values represented as mean ± SEM. One-way ANOVA with multiple comparisons (**B**).

occurs post-transcriptionally, consistent with a miRNA-mediated repression (Bristol and Rothstein, 1996). Thus, we focused on EAAT2 to test the model that miR-218 released from dying motor neurons is taken up by neighbouring glia, where it could functionally regulate glial cellular expression, potentially contributing to glial reactivity and ongoing neuronal damage in ALS patients and animal models.

MiR-218 regulates EAAT2 protein expression through binding to the 3′ UTR

The mouse EAAT2 3′ UTR contains six putative miR-218 binding sites, five of which are conserved in humans (Targetscan.org, Release 7.1) (Fig. 1A). To confirm that miR-218 can regulate the expression of EAAT2, we first performed luciferase assays with six EAAT2 3′ UTR constructs containing each of the putative miR-218 binding sites and one larger construct containing the four clustered binding sites in the distal end of the EAAT2 3′ UTR. The first site (UTR1) was predicted to have the best context score; however, this site only reduced the luminescence by 23%. The site in UTR2 had no effect on the luminescence. Intriguingly, when probed individually, the four distal sites did not affect the luminescence significantly; however, when probed as a cluster (UTR3abcd), these sites seem to act cooperatively, as they reduced the luminescence by 65% (Fig. 1B). It has been previously demonstrated that clustered miRNA sites can act cooperatively to repress target mRNA translation (Grimson *et al.*, 2007; Saetrom *et al.*, 2007), and because there are no polyA sites in between this cluster, these four binding sites will always be expressed together on the same transcript. Next, to determine whether miR-218 expression in astrocytes was sufficient for EAAT2 repression, we transiently transfected primary astrocytes with miR-218 or scrambled miRNA control and found that EAAT2 was selectively lost in the miR-218-transfected cells (Fig. 1C). These data suggest that miR-218 directly binds to the EAAT2 3′ UTR and is sufficient to repress its translation in astrocytes.

Healthy and ALS astrocytes in adult mice do not express miR-218

We and others recently found that miR-218 was a motor neuron-enriched miRNA in developing and adult motor

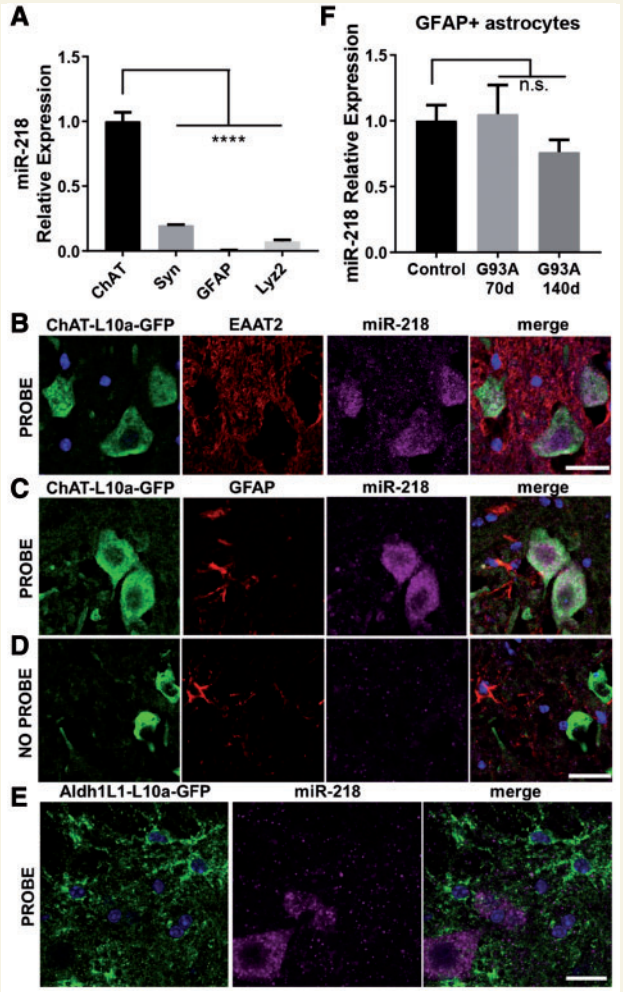

Figure 2 Wild-type and ALS astrocytes from adult mice do not express miR-218. (**A**) MiRAP data from Hoye *et al.* (2017) were plotted to demonstrate that miR-218 is specifically enriched in ChAT + motor neurons as compared to other CNS cell types in adult spinal cord tissue (ChAT = choline acetyltransferase, cholinergic neurons; Syn = synapsin 1, all neurons; Lyz2 = lysozyme M, microglia; GFAP = glial fibrillary acidic protein, astrocytes), including GFAP + astrocytes. *n* = 3/cell type. (**B**–**E**) MiR-218 *in situ* hybridizations indicate miR-218 is enriched in ChAT + motor neurons as compared to background (**D**; no probe) and EAAT2 +, GFAP + and ALDH1L1 + astrocytes in mouse spinal cord tissue. Scale bar = 25 μm. (**F**) MiRAP of tAgo2 derived from GFAP + astrocytes indicates miR-218 is not upregulated in astrocytes from the spinal cords of 70- and 140-day ALS SOD1G93A mice as compared to astrocytes from littermate LSL-tAgo2, GFAP Cre control mice. *n* = 3 (control), 3 (70-day SOD1G93A) and 6 (140-day SOD1G93A). Values represented as mean ± SEM. One-way ANOVA with multiple comparisons (**A** and **F**).

neurons (Amin *et al.*, 2015; Thiebes *et al.*, 2015; Hoye *et al.*, 2017). Furthermore, comparison to other CNS cell types indicated that miR-218 was over 150-fold more abundant in motor neurons than astrocytes in adult spinal cord tissue (Fig. 2A). Similarly, we performed miR-218 *in situ* hybridizations and confirmed the enrichment of miR-218 in choline acetyltransferase (ChAT) positive motor neurons as compared to EAAT2 + (Fig. 2B), glial fibrillary acidic protein (GFAP +; Fig. 2C) and aldehyde dehydrogenase 1 (ALDH1L1 +; Fig. 2E) astrocytes, as well as background (no probe; Fig. 2D). For ChAT and ALDH1L1 visualization, translating ribosome affinity purification reporter mice expressing GFP-tagged ribosomal L10a under these promoters were used (Doyle *et al.*, 2008). We also isolated EAAT2 promoter active cells from brain and spinal cord tissue by fluorescence-activated cell sorting at different developmental time points and found that miR-218 expression in astrocytes is detectable early in development, but negligible at postnatal Day 28 (P28) (Supplementary Fig. 1). Therefore, miR-218 may be expressed developmentally in astrocytes or astrocyte precursors, but adult astrocytes do not express significant amounts of miR-218. This suggests that miR-218 does not normally have the opportunity to target EAAT2 in adult astrocytes.

While miR-218 is not abundantly expressed in non-diseased adult astrocytes, it is possible that miR-218 is upregulated in ALS astrocytes. To directly assess the endogenous astrocytic miR-218, we used miRNA tagging and affinity purification (miRAP), in which mice expressing lox-stop-lox GFP-myc-tagged argonaute 2 (tAgo2) are crossed to mice expressing Cre recombinase under a cell type specific promoter, such as GFAP (He *et al.*, 2012; Hoye *et al.*, 2017). Immunoprecipitation of tAgo2 isolates only miRNA associated with tAgo2 expressed in GFAP + astrocytes. By crossing these mice to $SOD1^{G93A}$ ALS model mice, we were able to isolate miRNAs associated with tAgo2 derived from astrocytes during ALS disease. Using this approach, we found that miR-218 was not significantly changed in ALS astrocytes as compared to non-diseased littermate controls (Fig. 2F). These data demonstrate that miR-218 is expressed only at low levels in adult astrocytes, both wild-type and ALS. Therefore, these data argue against endogenous astrocyte-derived miR-218 as a regulator of protein expression in adult astrocytes.

Astrocytes take up extracellular miR-218 released from dying motor neurons

Our previous work found that motor neuron-enriched miR-218 is released extracellularly from dying and/or dysfunctional motor neurons in ALS model rats (Hoye *et al.*, 2017). We hypothesized that neighbouring astrocytes take up the miR-218 released from motor neurons in ALS, where miR-218 can regulate EAAT2 and potentially other astrocyte targets. However, there are many possible modes of uptake, and these may not be mutually exclusive. Therefore, to probe astrocytic uptake of extracellular, motor neuron-derived miR-218 without bias, we developed a miR-218 uptake sensor. Because miRNAs typically repress mRNA translation, most reporters, such as those in Fig. 1, function in an 'OFF' modality. A more desirable

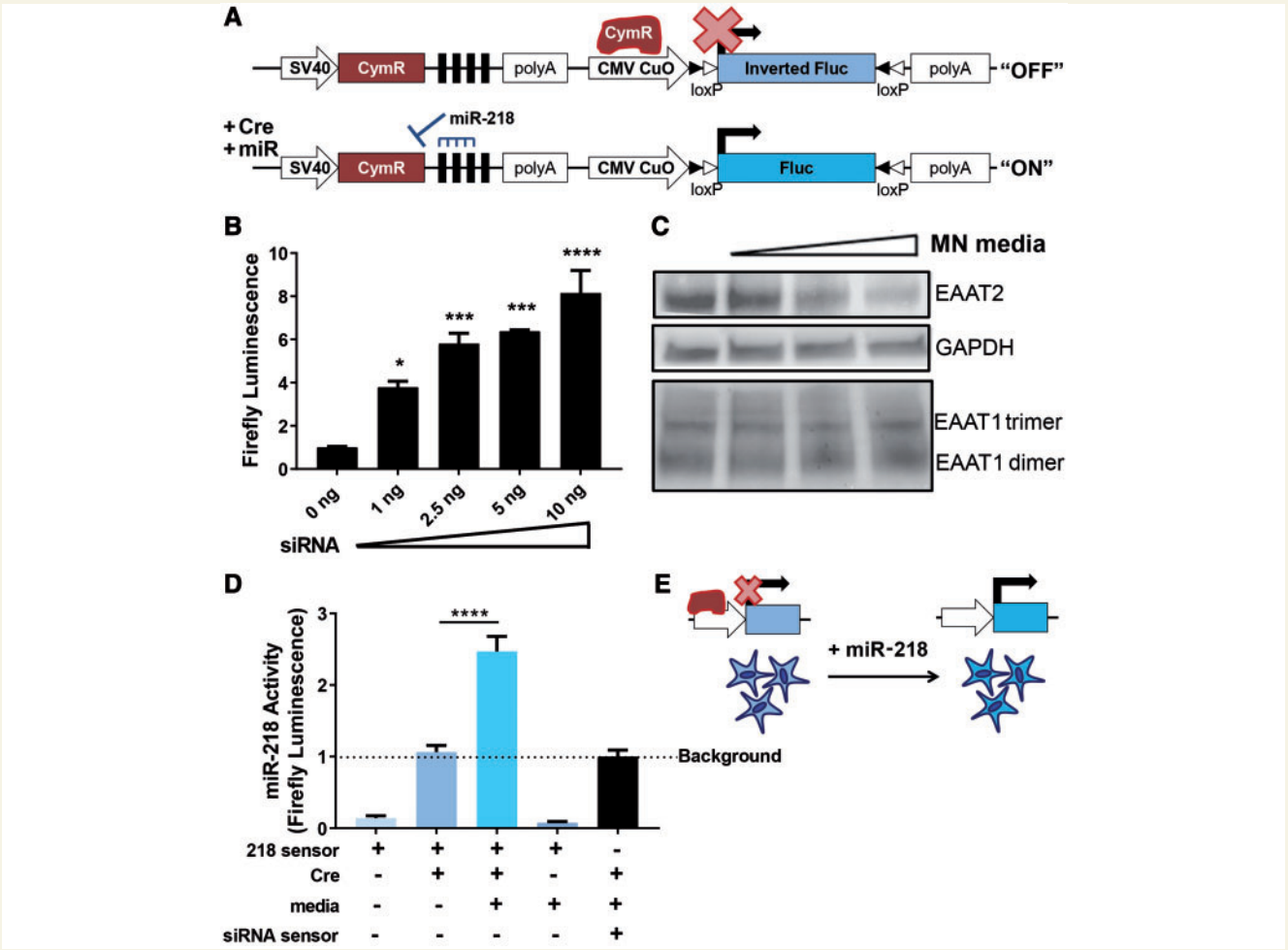

Figure 3 Astrocytes take up extracellular, motor neuron-derived miR-218. (**A**) An miR-218 uptake reporter based on the cumate gene switch, where RNAi binding sites (black rectangles) for miR-218 or siRNA to GFP (negative control) are placed downstream of CymR repressor protein. In the absence of miR-218/siRNA, CymR binds to the cumate operon (CuO) and represses downstream firefly luciferase (Fluc). When miR-218/siRNA are present, they repress CymR, thus allowing Fluc transcription. The Fluc has been inverted and floxed, such that it is Cre dependent. (**B**) HEK 293T cells transiently transfected with Cre and the siRNA to GFP-regulated sensor respond to increasing amounts of siRNA. *n* = 3 technical replicates/condition. (**C**) To model extracellular miR-218, media from lysed NSC-34 cells was applied to primary astrocytes. EAAT2, but not EAAT1, is selectively lost in a dose-dependent fashion. The monomer EAAT2 band (~60 kDa) is shown. (**D** and **E**) Primary astrocytes expressing the miR-218-regulated sensor, but not siRNA-regulated sensor, respond to lysed NSC-34 media in a Cre-dependent manner. *n* = 2–4 biological replicates with 3–4 technical replicates/assay. Values represented as mean ± SEM. One-way ANOVA with multiple comparisons (**B** and **D**).

sensor would function positively as an 'ON' system. Such an imaging modality, e.g. the RILES (RNAi-Inducible Luciferase Expression System) was previously designed by taking advantage of the cumate gene-switch (Mullick *et al.*, 2006). The cumate gene-switch functions like other repressor systems: the CymR repressor protein binds to the cumate operon, thus inhibiting expression of the downstream firefly luciferase (Fluc). In the presence of an inducer, cumate, the conformation of CymR is changed such that it can no longer bind to the cumate operon, thus allowing expression of Fluc. The RILES method takes advantage of the cumate gene switch by placing the CymR repressor under the control of an endogenous RNAi, rather than cumate (Ezzine *et al.*, 2013). In this manner, the cumate operon will be active when the RNAi of interest represses CymR expression (Fig. 3A). To enhance the control of expression, we have also floxed the downstream luciferase with loxP sites and inverted the luciferase, such that it is Cre dependent. As a negative control, we made a siRNA tGFP-regulated sensor that will have only background luminescence in the absence of siRNA to GFP.

We validated that the sensor was responsive to siRNA in a dose-dependent fashion *in vitro* (Fig. 3B). To model motor neuron loss and subsequent release of miR-218, we cultured primary astrocytes with media from NSC-34 cells, a fusion of a neuroblastoma cell line and mouse spinal cord cells (Cashman *et al.*, 1992). While NSC-34 cells are not the perfect model of motor neurons, they do

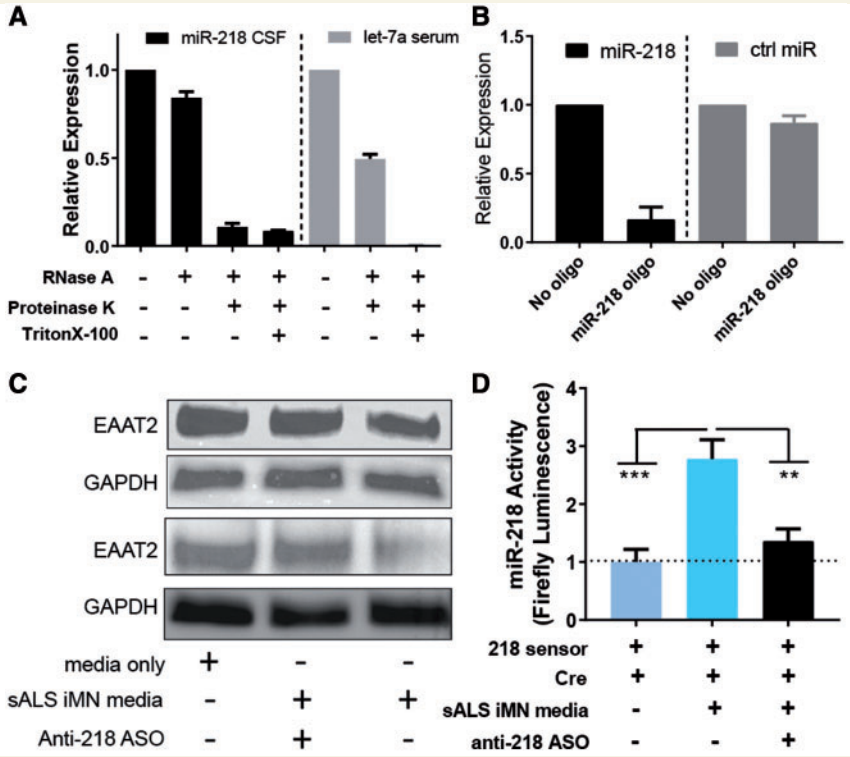

Figure 4 Extracellular, motor neuron-derived miR-218 is protein-bound and its activity can be blocked using ASOs. (**A**) ALS end-stage rat model CSF was treated with RNase A, proteinase K and Triton™ X-100. Treatment with RNase A only degrades free miR-218 (~15% of total). Treatment with proteinase K followed by RNase A degrades free and protein-bound miR-218 (~80% of total). Treatment with Triton™ X-100, to solubilize vesicles, followed by proteinase K and RNase A has no further effect on the miR-218 signal. Conversely, treatment of rat serum with proteinase K followed by RNase A degrades only ~50% of let-7a, whereas pretreatment with Triton™ X-100 results in 100% loss of the let-7a signal. n = 3–4/condition. (**B**) Biotinylated anti-miR-218 oligonucleotides can precipitate miR-218, but not control miRNA 103a-3p, from ALS rat model CSF. n = 2/condition. Each trial was normalized to the corresponding no oligonucleotide control. (**C**) Treatment of primary astrocytes with media from sporadic ALS patient (sALS) iPSC-derived motor neurons (iMNs) results in loss of EAAT2 protein, but can be mitigated by addition of anti-miR-218 ASOs. n = 3. (**D**) Primary astrocytes expressing the miR-218 uptake sensor also respond to iPSC-derived motor neuron media, and this response is mitigated by anti-miR-218 ASOs. n = 3 Biological replicates with 2–4 technical replicates/assay. Values represented as mean ± SEM. One-way ANOVA with multiple comparisons (**D**).

express ChAT, a motor neuron marker, and importantly, miR-218. To this end, we added media from lysed NSC-34 cells and found that EAAT2 protein levels were lost in a dose-dependent fashion, whereas EAAT1 protein was not affected (Fig. 3C). Using this model of motor neuron loss, we tested whether astrocytes expressing our miR-218 sensor would respond to miR-218 containing media. To establish the background luminescence activity associated with the sensor, we found that Cre− astrocytes had virtually no luminescence activity, whereas Cre+ astrocytes had measurable luminescence. Thus, the miR-218 sensor expressing astrocytes transfected with Cre represent the background luminescence activity of the sensor. When miR-218 sensor-expressing astrocytes are transfected with Cre and subsequently exposed to miR-218 containing media, the luminescence activity increases by nearly 3-fold (Fig. 3D). This increase is dependent on Cre, as astrocytes expressing the miR-218 regulated sensor, but not Cre, do not respond to miR-218 containing media (Fig. 3D). Similarly, astrocytes expressing a control sensor regulated by a siRNA to GFP do not respond to miR-218 containing media, suggesting the increase in luminescence of the miR-218 sensor-expressing astrocytes is related to miR-218 uptake and activity (Fig. 3D). Notably, the luminescence activity of the siRNA sensor exposed to miR-218 containing media is similar to the luminescence activity of the miR-218 sensor not exposed to media, confirming this luminescence is background activity.

Extracellular miR-218 is largely protein-bound and capable of binding oligonucleotides

If motor neuron-derived miR-218 is taken up by neighbouring astrocytes and deleteriously regulating their expression, blocking miR-218 uptake could be beneficial in ALS. However, because the mode of miR-218 uptake is unknown, we reasoned that understanding the extracellular state of miR-218 would provide insight into blocking its activity. The field of extracellular miRNAs has grown

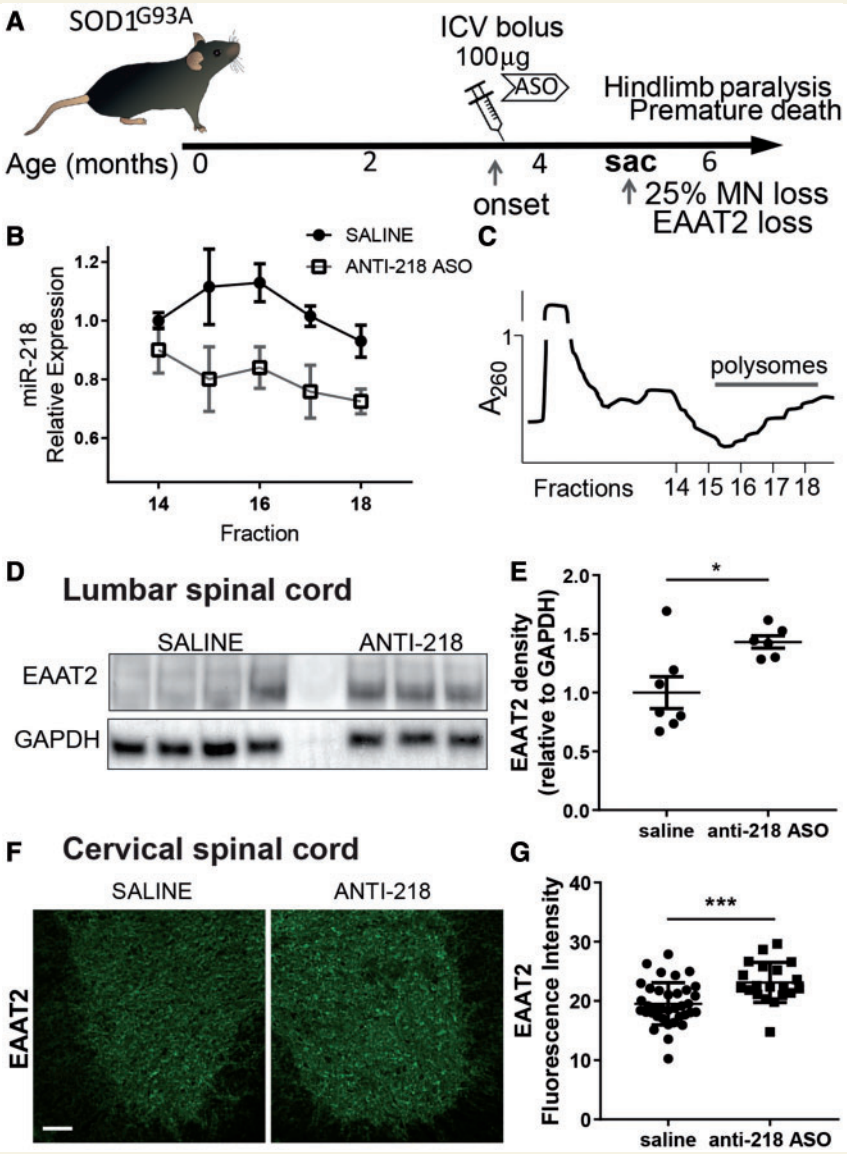

Figure 5 Blocking miR-218 mitigates EAAT2 loss in ALS model mice. (**A**) SOD1G93A mice were treated with miR-218 ASOs or saline via ICV injection at 110 days, which is post-disease onset. n = 6–7/group (two cohorts of 3–4 mice/group). (**B** and **C**) Polysomes were isolated from the brainstems of treated mice at 140 days to check for miR-218 inhibition. Polysome-containing fractions from miR-218 ASO-treated mice have less miR-218, indicating it is excluded from these fractions as compared to saline-treated mice, consistent with miR-218 inhibition. n = 4/treatment. (**D**–**G**) Mice treated with miR-218 ASOs have preserved EAAT2 as compared to saline-treated mice in both the lumbar (**D** and **E**) and cervical (**F** and **G**) spinal cords, as assessed by immunoblot (**D** and **E**) and immunofluorescence (**F** and **G**), respectively. n = 6–7/group (two cohorts of 3–4 mice/group) (**D** and **E**) and n = 3–5/group with 6–8 sections/mouse (**F** and **G**). The monomer EAAT2 band (~60 kDa) is shown in (**D**). Images in (**F**) were taken such that no saturation occurred for quantitation and then equivalently brightened for demonstrative purposes. Scale bar = 100 µm. Values represented as mean ± SEM. Student's unpaired, two-tailed t-test (**E** and **G**) with Benjamini-Hochberg correction for multiple comparisons (FDR < 0.1). Adjusted P-values: *$P \leqslant 0.05$, **$P \leqslant 0.01$, ***$P \leqslant 0.001$.

extensively since they were first measured in blood plasma and serum (Chim *et al.*, 2008; Lawrie *et al.*, 2008). While there is increasing evidence that extracellular miRNAs can be encapsulated in vesicles, the majority are protein-associated (Arroyo *et al.*, 2011; Turchinovich *et al.*, 2011). To determine whether extracellular CSF miR-218 was free, protein-bound or encapsulated in vesicles, we performed RNase A digestion followed by proteinase K digestion. MiRNAs encapsulated in vesicles will be protected from both RNase A and proteinase K, whereas miRNAs associated with protein will be resistant to RNase A degradation, but can be sensitized by first treating with proteinase K (Arroyo *et al.*, 2011; Turchinovich *et al.*, 2011). As compared to the total, RNase A digestion resulted in ~15% loss of the miR-218 signal in rat CSF (Fig. 4A), suggesting 15% of extracellular miR-218 is free. Treating rat CSF with proteinase K followed by RNase A ablated nearly all of the miR-218 signal (Fig. 4A). Pretreatment

with Triton^{TM} X-100 to permeabilize membranes did not have any additional effect. These data suggest that the majority of miR-218 is protein-bound and not encapsulated in vesicles. In contrast, let-7a has been shown to be encapsulated in vesicles in serum and thus, protected from RNases and proteinases (Arroyo *et al.*, 2011). Indeed, we found that ~50% of let-7a in rat serum was protected from proteinase K followed by RNase A digestion, but this signal was lost upon pretreatment with Triton^{TM} X-100 (Fig. 4A), consistent with let-7a in serum being encapsulated in vesicles.

Because extracellular miR-218 is largely protein-bound, these data suggest that its activity in astrocytes could be blocked by ASOs. To determine whether extracellular miR-218 is capable of binding oligonucleotides, we precipitated it from rat CSF using anti-miR-218 oligonucleotides. Extracellular miR-218 is ~5-fold depleted from rat CSF using anti-miR-218 oligonucleotides as compared to precipitation with no oligonucleotides (Fig. 4B). Conversely, a control miRNA (miR-103a-3p) is not precipitated from rat CSF using anti-miR-218 oligonucleotides (Fig. 4B). These data demonstrate that extracellular miR-218 can bind oligonucleotides, suggesting the activity of extracellular, motor neuron-derived miR-218 can be blocked with ASOs.

To test whether the effect of motor neuron-derived miR-218 on astrocytic EAAT2 could be mitigated using ASOs, we applied media from sporadic ALS patient iPSC-derived motor neurons to primary astrocytes. This miR-218 containing media resulted in loss of EAAT2 protein, but EAAT2 repression was greatly mitigated by application of anti-miR-218 ASO (Fig. 4C). Moreover, anti-miR-218 ASOs also mitigated the responsiveness of astrocytes expressing the miR-218 uptake sensor (Fig. 4D). Together, these data support the conclusion that extracellular, motor neuron-derived miR-218 can directly contribute to EAAT2 loss in astrocytes and its activity can be blocked using ASOs.

Inhibition of miR-218 mitigates EAAT2 loss in ALS model mice

Because the effect of motor neuron-derived miR-218 on astrocytic EAAT2 can be blocked using ASOs *in vitro*, we reasoned that we could test this model in ALS rodents. We and others have previously used ASOs to inhibit miRNAs *in vivo* (Koval *et al.*, 2013; Butovsky *et al.*, 2015). Bolus intracerebroventricular (ICV) delivery of 100–400 µg of these ASOs results in widespread distribution throughout the CNS, including spinal cord (DeVos and Miller, 2013*a*).

In our ALS model mice, which are on a congenic BL6 background, miR-218 is significantly depleted in whole spinal cord by 126 days, with detectable loss starting around 100 days (Hoye *et al.*, 2017). Because miR-218 is released from dying motor neurons beginning around the time of disease onset, we wanted to deliver anti-miR-218 ASOs post-onset. Thus, we delivered either saline or 100 µg anti-miR-218 ASOs to SOD1^{G93A} mice at 110 days and sacrificed them 30 days post-treatment to test for miR-218 inhibition and EAAT2 preservation (Fig. 5A). First, we performed polysome profiling to determine whether miR-218 was inhibited as measured by its exclusion from polysome fractions (Androsavich *et al.*, 2016). We found that anti-miR-218 ASO-treated mice had ~20–50% miR-218 exclusion in polysome-containing fractions (Fig. 5B and C), indicating the anti-miR-218 ASOs were successfully inhibiting miR-218. In mice treated with anti-miR-218, we also found that EAAT2 protein levels were maintained relative to saline-treated littermate controls by both immunoblot and immunofluorescence in the lumbar and cervical spinal cord, respectively (Fig. 5D–G). These data establish that miR-218 derived from dying motor neurons is taken up by neighbouring astrocytes *in vivo* and is sufficient to directly mediate changes in astrocytic expression that are characteristic of ALS, such as loss of EAAT2.

Translated mRNAs downregulated in ALS astrocytes contain miR-218 binding sites and are de-repressed upon miR-218 inhibition

We initially focused on miR-218's downregulation of EAAT2 because of strong support for EAAT2 loss and subsequent excitotoxicity in both human and rodent models of ALS. However, numerous astrocytic proteins are dysregulated in ALS. Thus, to determine whether motor neuron-derived miR-218 may be responsible for downregulating additional targets in ALS astrocytes, we used previously reported translating ribosome affinity purification data from astrocytes in ALS model mice (Sun *et al.*, 2015). Indeed, using two miRNA target prediction algorithms, miRDB and TargetScan, we found that 12% and 17%, respectively, of the downregulated transcripts in ALS astrocytes were putative miR-218 targets (Table 1). However, sites for pan-neuronally-enriched miRNAs (Hoye *et al.*, 2017), miR-431 and miR-382, were not abundant in downregulated transcripts in ALS astrocytes (Table 1). This significant enrichment [$P = 0.009$ (miRDB) and $P = 0.003$ (TargetScan)] in miR-218 binding sites in transcripts translationally downregulated in ALS astrocytes is consistent with our EAAT2 findings. To confirm these putative miR-218 targets, we performed reverse transcription-quantitative PCR on the polysome profiling RNA (from Fig. 5B) and found that each of the five targets tested were de-repressed upon miR-218 inhibition as compared to saline-treated mice (Fig. 6). Moreover, non-miR-218 targets were not affected by miR-218 inhibition (Fig. 6), confirming the specificity of miR-218-mediated regulation. These data indicate motor neuron-derived miR-218 is broadly affecting astrocyte protein expression and cellular state in neurodegeneration.

Table 1 Numerous translated mRNAs downregulated in ALS astrocytes are putative miR-218 targets and de-repressed upon miR-218 inhibition

MiRNA target prediction algorithm	Putative miRNA targets downregulated in ALS astrocytes	% Overlap	*P*-value
miRDB: miR-218	*Mbnl1*, *Anks1b*, *Sertad2*, *Ppargc1a*, *Olig2*	12.2 (5/41)	0.009
TargetScan: miR-218	*Tcf12*, *Mbnl1*, *Nfix*, *Anks1b*, *Sertad2*, *Cpeb2*, *Ppargc1a*	17.1 (7/41)	0.003
miRDB: miR-431	None	0 (0/41)	1.00
TargetScan: miR-431	*Fbxo32*	2.44 (1/41)	0.726
miRDB: miR-382	*Mbnl1*, *Trim59*	4.88 (2/41)	0.147
TargetScan: miR-382	*Mbnl1*, *Fam84b*	4.88 (2/41)	0.162

Using previously generated translating ribosome affinity purification data from ALS astrocytes (Sun *et al.*, 2015) and two different miRNA target prediction algorithms, miRDB and TargetScan, we determined that 12.2% and 17%, respectively, of translationally downregulated mRNAs in ALS astrocytes (41 transcripts total) were putative miR-218 targets. However, sites for two pan-neuronally-enriched miRNAs (Hoye *et al.*, 2017), miR-431 and miR-382, were not significantly represented in mRNAs translationally downregulated in ALS astrocytes. Fisher's exact test was used to determine statistical significance with Bonferroni correction for multiple (three) comparisons.

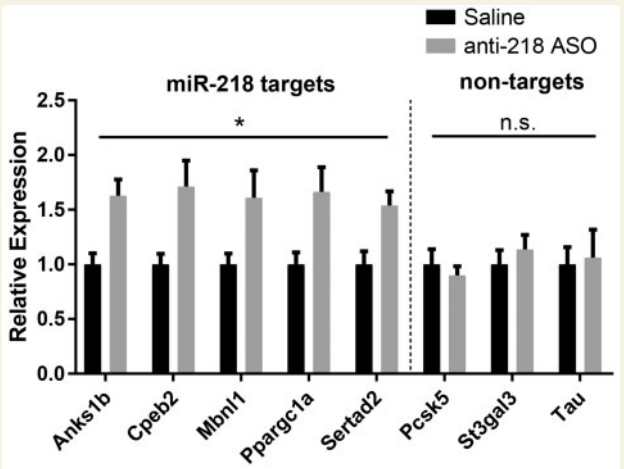

Figure 6 Putative miR-218 targets that are translationally downregulated in ALS astrocytes are de-repressed upon miR-218 inhibition. RT-qPCR of RNA obtained from polysome profiles of SOD1G93A mouse brainstems treated with saline or anti-218 ASOs indicates that putative miR-218 targets are de-repressed following anti-218 ASO treatment. $n = 4$/group. Conversely, non-miR-218 targets are not de-repressed upon anti-218 ASO treatment. $n = 4$/group. Student's unpaired, two-tailed *t*-test with Benjamini-Hochberg correction for multiple comparisons (FDR < 0.1). Adjusted *P*-values: $^*P \leqslant 0.1$.

Inhibition of motor neuron-derived miR-218 mitigates astrogliosis in ALS model mice

Throughout neurodegenerative disease progression, glia can lose their homeostatic function (Van Damme *et al.*, 2007; Cassina *et al.*, 2008; Ferraiuolo *et al.*, 2011; Madji Hounoum *et al.*, 2017) and adopt a reactive phenotype (Butovsky *et al.*, 2014; Endo *et al.*, 2015; Almad *et al.*, 2016; Liddelow *et al.*, 2017). Because miR-218 contributes to the loss of EAAT2 and potentially other homeostatic astrocytic proteins, we tested whether inhibition of miR-218 derived from dying motor neurons would also mitigate this conversion to reactive astrocytes. It was recently demonstrated that connexin 43 (Cx43), a gap junction and hemi-channel protein, is upregulated in ALS and that antagonizing its hemichannel activity prevented astrocyte-induced motor neuron loss (Almad *et al.*, 2016). Intriguingly, several reports have found that modulating EAAT2 expression inversely affects Cx43 expression (Unger *et al.*, 2012; Hussein *et al.*, 2016). Likewise, we found that our anti-miR-218 ASO-treated mice had not only restored EAAT2 expression, but the upregulation of Cx43, and also GFAP, had been mitigated (Fig. 7A–H). Overall, these data support the model that miR-218 released from dying motor neurons can lead to loss of homeostatic protein expression, such as EAAT2, and astrogliosis.

Discussion

We demonstrate here that extracellular miR-218 released from dying motor neurons in ALS can be taken up by neighbouring astrocytes and negatively affect astrocyte function. We were able to establish this surprising link between motor neurons and glia by focusing on EAAT2, a glutamate transporter expressed by astrocytes, which has numerous highly conserved miR-218 binding sites in the 3′ UTR. We confirmed that astrocytes can take up extracellular, motor neuron-derived miR-218 *in vitro* and that inhibition of miR-218 mitigates EAAT2 loss and other miR-218-mediated changes in ALS model mice. The post-transcriptional loss of EAAT2 had already been established in both ALS patients and rodent models (Rothstein *et al.*, 1995; Bristol and Rothstein, 1996; Howland *et al.*, 2002), making it an attractive candidate to validate the functionality of motor neuron-derived miR-218 in astrocytes. Uptake of neuronally-derived miRNAs by neighbouring glia and their downstream, negative consequences establishes a novel mechanism of neurodegeneration.

Neuronal cell loss is a unifying theme in neurodegeneration and it is recognized that neuronal injury leads to a response from the surrounding glia. While the homeostatic role of glia in the CNS involves clearance of cellular debris and metabolites through phagocytosis, it is known that in

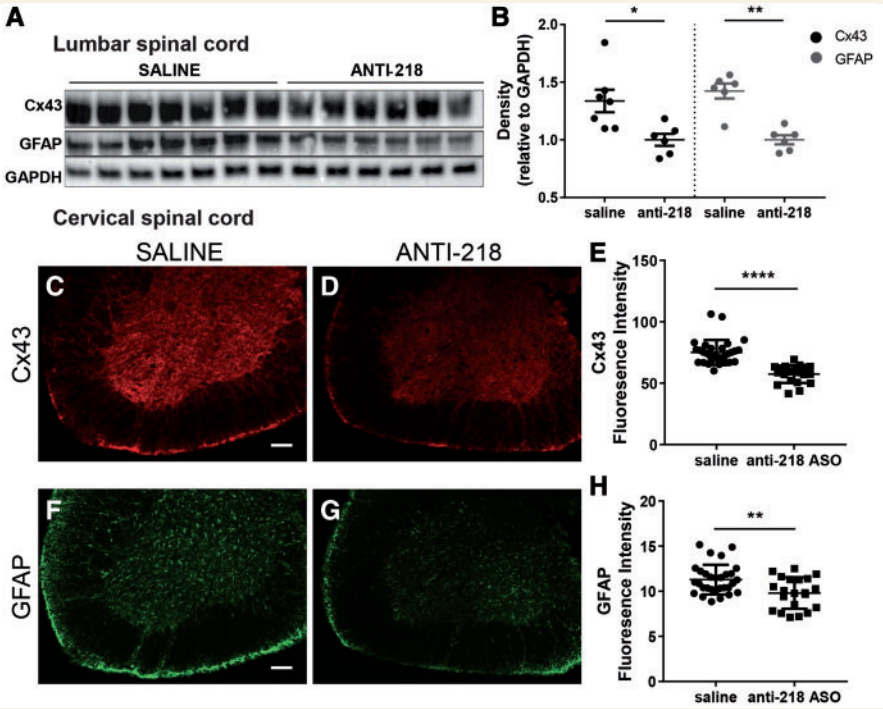

Figure 7 Blocking miR-218 mitigates astrogliosis in ALS model mice. (**A**–**H**) Mice treated with miR-218 ASOs have reduced expression of both Cx43 and GFAP, markers of astrogliosis, as compared to saline-treated mice in both the lumbar (**A** and **B**) and cervical (**C**–**H**) spinal cords, as assessed by immunoblot (**A** and **B**) and immunofluorescence (**C**–**H**), respectively. n = 6–7/group (two cohorts of 3–4 mice/group) (**A** and **B**) and n = 3–5/group with 8–10 sections/mouse (**C**–**H**). Images in (**C**, **D**, **F** and **G**) were taken such that no saturation occurred for quantitation and then equivalently brightened for demonstrative purposes. Scale bar = 100 μm. Values represented as mean ± SEM. Student's unpaired, two-tailed t-test (**B**, **E** and **H**) with Benjamini-Hochberg correction for multiple comparisons (FDR < 0.1). Adjusted P-values: $^{*}P \leqslant 0.05$, $^{**}P \leqslant 0.01$, $^{***}P \leqslant 0.001$, $^{****}P \leqslant 0.0001$.

neurodegeneration, glia can become reactive (Butovsky *et al.*, 2014; Liddelow *et al.*, 2017). This glial reactivity may be beneficial at some point; however, chronic glial reactivity often leads to loss of homeostatic function and is deleterious to the survival of the remaining neurons. Our work uncovers a novel mechanism for understanding how the glial response to neuronal injury in the CNS can be mediated directly by signalling molecules released by dying neurons in a manner that maintains their functionality. We speculate that this mechanism of release of functional signalling molecules may be broadly applicable in neurodegeneration, and moreover, the causative neuronal signalling components could be different for various diseases.

While possible that many components of a dying or damaged neuron could have deleterious signalling consequences in neighbouring glia, miRNAs may be particularly enabled to signal to recipient cells. Extracellular miRNAs are unusually stable in biological fluids, due to their encapsulation in vesicles and/or association with proteins (Hunter *et al.*, 2008; Arroyo *et al.*, 2011; Turchinovich *et al.*, 2011), and it has been established that extracellular miRNAs can be taken up and function in recipient cells in both physiological (Valadi *et al.*, 2007; Wang *et al.*, 2010) and pathological states (Mittelbrunn *et al.*, 2011; Fabbri *et al.*, 2012; Lehmann *et al.*, 2012). However, the majority of these studies have been performed in cell culture models using purified miRNA-containing vesicles. Our work describes the function of an abundant, motor neuron-derived miRNA that naturally exhibits nearly 10-fold elevation in the CSF of end-stage ALS model rats (Hoye *et al.*, 2017). Our demonstration that blocking miR-218 activity with ASOs mitigates miR-218-mediated changes in an ALS model provides important evidence for cell-to-cell communication *in vivo* in the CNS. Moreover, this mechanism could be widely applicable to disease states, as miRNAs are released from cells subsequent to injury (Corsten *et al.*, 2010; Zhang *et al.*, 2010), and it is likely that these miRNAs also maintain their regulatory capacity and could similarly function as signalling molecules in neighbouring cells. It was recently demonstrated that miR-21 is released in response to peripheral nerve injury (Simeoli *et al.*, 2017); however, we predict that the role of extracellular miRNAs released subsequent to injury is largely underappreciated. Moreover, this signalling could occur in multiple cell types with unique downstream consequences.

One of the striking aspects of most ALS is rapid decline after the first symptoms and contiguous neuronal loss (Ravits *et al.*, 2007). This precipitous decline may suggest a failure of homeostatic mechanisms or may imply one or more feed forward loops that worsen an already damaged

system. The recognition that progression rates in ALS and other neurodegenerative diseases are non-cell autonomous (Ilieva *et al.*, 2009) suggests non-neuronal cells may be one potential feed forward loop. Our work supports a model in which a focal neuronal injury could lead to a response from surrounding glia that causes loss of homeostatic glial function and increased reactivity, which ultimately exacerbates neuronal degeneration. Further neuronal injury would lead to increased extracellular miR-218, which would continue to worsen astrocyte dysfunction, thus accelerating the vicious cycle. Moreover, as miR-218 is increased in the CSF of ALS model rats, it is possible that the CSF serves as a conduit for this feedforward process to spread along the spinal cord. Indeed, it has been previously demonstrated that application of ALS patient CSF to cultured astrocytes results in toxicity and loss of EAAT2 protein (Shobha *et al.*, 2007).

Intervening in miR-218-mediated astrocyte dysfunction has exciting and broad therapeutic implications. However, our current approach is not amenable to adequately testing whether miR-218 inhibition in astrocytes extends survival in ALS, as currently, we are limited by our inability to selectively target miR-218 signalling in astrocytes. It was recently demonstrated that genetic ablation of miR-218 in mice resulted in motor neuron degeneration (Amin *et al.*, 2015); thus, our current approach as a treatment could have potentially deleterious effects in motor neurons that would confound our analysis. Nevertheless, we remain enthusiastic that selectively targeting miR-218 in astrocytes will be feasible in the near future: it has already been demonstrated that ASOs can be specifically targeted to liver cells by conjugating the ASOs with a ligand that is recognized by liver-specific receptors (Prakash *et al.*, 2014). Therefore, targeting of astrocytes may be a feasible future application of miR-218 inhibitors.

This work also raises the interesting question of the physiological role of EAAT2 repression by miR-218. The conserved miR-218 binding sites in the EAAT2 3′ UTR suggest that this regulation may take place physiologically. One intriguing possibility is that during synaptic pruning, miR-218 is released from motor neuron synapses that are destined to be ablated. The loss of EAAT2 in neighbouring astrocytes would lead to excitoxicity in these motor neurons and accelerate their ablation. Alternatively, developmentally, postnatal Day 2.5 astrocytes express ~10-fold more miR-218 than adult astrocytes (Supplementary Fig. 1). This is still considerably less than motor neurons, but perhaps endogenous astrocytic miR-218 functions to repress EAAT2 developmentally while synaptic connections are being made. This may also contribute to the lower levels of EAAT2 in primary astrocytes harvested from pups. Thus, miR-218 may have a cryptic role in normal astrocyte development that maintains the conservation of miR-218 binding sites in astrocyte-derived sequences, yet this conserved role is co-opted during disease with deleterious consequences.

Our work defines a novel mechanism whereby miRNAs released from dying motor neurons can contribute to astrocyte dysfunction in neurodegeneration. This work clarifies the role of neuronal damage in eliciting a response from neighbouring glia, demonstrating that neuronally-derived miRNAs can exert functional changes in glia that contribute to disease. Finally, this mechanism is consistent with the non-cell autonomous nature of neurodegenerative diseases and may also provide insight into how this feed-forward process is initiated.

Acknowledgements

We thank Dr. Len Maggi and Dr. Jason Weber for assistance with polysome profiling. We thank Dr. Patrick Baril for the RILES plasmid. We also thank Dr. Azad Bonni for his helpful critique of this work. We thank Dr. Amber Salter for reviewing the statistical methods and Erika Jaques for assisting with manuscript preparation. Thank you to Elena Fisher for preparing the thumbnail schematic.

Funding

This work was supported by Project5 for ALS to T.M.M.; Target ALS to T.M.M.; the National Institute of Neurological Disorders and Stroke [K08NS074194 and R01NS078398 to T.M.M., F31NS092340 to M.L.H.]; the Robert Packard Center for ALS Research to T.M.M.; and the University of Missouri Spinal Cord Injury/Disease Research Program to T.M.M., and the Hope Center for Neurological Disorders. L.A.J. was supported by NIH T35 NHLBI training grant (T35 HL007815). J.D.D. is supported in part by a NARSAD Independent Investigator grant from the Brain and Behavior Research Foundation and R01 NS102272. This work was also supported by access to equipment made possible by the Hope Center for Neurological Disorders, and the Departments of Neurology and Psychiatry at Washington University School of Medicine. Immunofluorescence images were acquired on a Nikon A1Rsi confocal microscope through the use of the Washington University Center for Cellular Imaging (WUCCI) supported by Washington University School of Medicine, The Children's Discovery Institute of Washington University and St. Louis Children's Hospital, the Foundation for Barnes-Jewish Hospital and the National Institute for Neurological Disorders and Stroke (NS086741).

Competing interests

Washington University has filed patents regarding miRNA as biomarkers and therapeutic targets for ALS. The authors declare no other competing financial interests.

Supplementary material

Supplementary material is available at *Brain* online.

References

Almad AA, Doreswamy A, Gross SK, Richard JP, Huo YQ, Haughey N, et al. Connexin 43 in astrocytes contributes to motor neuron toxicity in amyotrophic lateral sclerosis. Glia 2016; 64: 1154–69.

Ambros V. The functions of animal microRNAs. Nature 2004; 431: 350–5.

Amin ND, Bai G, Klug JR, Bonanomi D, Pankratz MT, Gifford WD, et al. Loss of motoneuron-specific microRNA-218 causes systemic neuromuscular failure. Science 2015; 350: 1525–9.

Androsavich JR, Sobczynski DJ, Liu X, Pandya S, Kaimal V, Owen T, et al. Polysome shift assay for direct measurement of miRNA inhibition by anti-miRNA drugs. Nucleic Acids Res 2016; 44: e13.

Arroyo JD, Chevillet JR, Kroh EM, Ruf IK, Pritchard CC, Gibson DF, et al. Argonaute2 complexes carry a population of circulating microRNAs independent of vesicles in human plasma. Proc Natl Acad Sci USA 2011; 108: 5003–8.

Bajenaru ML, Zhu Y, Hedrick NM, Donahoe J, Parada LF, Gutmann DH. Astrocyte-specific inactivation of the neurofibromatosis 1 gene (NF1) is insufficient for astrocytoma formation. Mol Cell Biol 2002; 22: 5100–13.

Boillee S, Yamanaka K, Lobsiger CS, Copeland NG, Jenkins NA, Kassiotis G, et al. Onset and progression in inherited ALS determined by motor neurons and microglia. Science 2006; 312: 1389–92.

Bristol LA, Rothstein JD. Glutamate transporter gene expression in amyotrophic lateral sclerosis motor cortex. Ann Neurol 1996; 39: 676–9.

Butovsky O, Jedrychowski MP, Cialic R, Krasemann S, Murugaiyan G, Fanek Z, et al. Targeting miR-155 restores abnormal microglia and attenuates disease in SOD1 mice. Ann Neurol 2015; 77: 75–99.

Butovsky O, Jedrychowski MP, Moore CS, Cialic R, Lanser AJ, Gabriely G, et al. Identification of a unique TGF-beta dependent molecular and functional signature in microglia. Nat Neurosci 2014; 17: 131–43.

Cashman NR, Durham HD, Blusztajn JK, Oda K, Tabira T, Shaw IT, et al. Neuroblastoma x spinal cord (NSC) hybrid cell lines resemble developing motor neurons. Dev Dyn 1992; 194: 209–21.

Cassina P, Cassina A, Pehar M, Castellanos R, Gandelman M, de Leon A, et al. Mitochondrial dysfunction in SOD1G93A-bearing astrocytes promotes motor neuron degeneration: prevention by mitochondrial-targeted antioxidants. J Neurosci 2008; 28: 4115–22.

Chim SS, Shing TK, Hung EC, Leung TY, Lau TK, Chiu RW, et al. Detection and characterization of placental MicroRNAs in maternal plasma. Clin Chem 2008; 54: 482–90.

Corsten MF, Dennert R, Jochems S, Kuznetsova T, Devaux Y, Hofstra L, et al. Circulating MicroRNA-208b and MicroRNA-499 reflect myocardial damage in cardiovascular disease. Circ Cardiovasc Genet 2010; 3: 499–506.

DeVos SL, Miller TM. Antisense oligonucleotides: treating neurodegeneration at the level of RNA. Neurotherapeutics 2013a; 10: 486–97.

DeVos SL, Miller TM. Direct intraventricular delivery of drugs to the rodent central nervous system. J Vis Exp 2013b; 75: e50326.

Doyle JP, Dougherty JD, Heiman M, Schmidt EF, Stevens TR, Ma G, et al. Application of a translational profiling approach for the comparative analysis of CNS cell types. Cell 2008; 135: 749–62.

Endo F, Komine O, Fujimori-Tonou N, Katsuno M, Jin S, Watanabe S, et al. Astrocyte-derived TGF-beta1 accelerates disease progression in ALS mice by interfering with the neuroprotective functions of microglia and T cells. Cell Rep 2015; 11: 592–604.

Ezzine S, Vassaux G, Pitard B, Barteau B, Malinge JM, Midoux P, et al. RILES, a novel method for temporal analysis of the in vivo regulation of miRNA expression. Nucleic Acids Res 2013; 41: e192.

Fabbri M, Paone A, Calore F, Galli R, Gaudio E, Santhanam R, et al. MicroRNAs bind to Toll-like receptors to induce prometastatic inflammatory response. Proc Natl Acad Sci USA 2012; 109: E2110–16.

Ferraiuolo L, Higginbottom A, Heath PR, Barber S, Greenald D, Kirby J, et al. Dysregulation of astrocyte-motoneuron cross-talk in mutant superoxide dismutase 1-related amyotrophic lateral sclerosis. Brain 2011; 134: 2627–41.

Gallardo G, Barowski J, Ravits J, Siddique T, Lingrel JB, Robertson J, et al. An alpha2-Na/K ATPase/alpha-adducin complex in astrocytes triggers non-cell autonomous neurodegeneration. Nat Neurosci 2014; 17: 1710–19.

Grimson A, Farh KK, Johnston WK, Garrett-Engele P, Lim LP, Bartel DP. MicroRNA targeting specificity in mammals: determinants beyond seed pairing. Mol Cell 2007; 27: 91–105.

Guerreiro R, Wojtas A, Bras J, Carrasquillo M, Rogaeva E, Majounie E, et al. TREM2 Variants in Alzheimer's disease. N Engl J Med 2013; 368: 117–27.

He M, Liu Y, Wang X, Zhang MQ, Hannon GJ, Huang ZJ. Cell-type-based analysis of MicroRNA profiles in the mouse brain. Neuron 2012; 73: 35–48.

Howland DS, Liu J, She YJ, Goad B, Maragakis NJ, Kim B, et al. Focal loss of the glutamate transporter EAAT2 in a transgenic rat model of SOD1 mutant-mediated amyotrophic lateral sclerosis (ALS). Proc Natl Acad Sci USA 2002; 99: 1604–9.

Hoye ML, Koval ED, Wegener AJ, Hyman TS, Yang CR, O'Brien DR, et al. MicroRNA profiling reveals marker of motor neuron disease in ALS models. J Neurosci 2017; 37: 5574–86.

Hunter MP, Ismail N, Zhang X, Aguda BD, Lee EJ, Yu L, et al. Detection of microRNA expression in human peripheral blood microvesicles. PLoS One 2008; 3: e3694.

Hussein AM, Ghalwash M, Magdy K, Abulseoud OA. Beta lactams antibiotic ceftriaxone modulates seizures, oxidative stress and connexin 43 expression in hippocampus of pentylenetetrazole kindled rats. J Epilepsy Res 2016; 6: 8–15.

Ilieva H, Polymenidou M, Cleveland DW. Non-cell autonomous toxicity in neurodegenerative disorders: ALS and beyond. J Cell Biol 2009; 187: 761–72.

Jonsson T, Stefansson H, Steinberg S, Jonsdottir I, Jonsson PV, Snaedal J, et al. Variant of TREM2 associated with the risk of Alzheimer's disease. N Engl J Med 2013; 368: 107–16.

Klipper-Aurbach Y, Wasserman M, Braunspiegel-Weintrob N, Borstein D, Peleg S, Assa S, et al. Mathematical formulae for the prediction of the residual beta cell function during the first two years of disease in children and adolescents with insulin-dependent diabetes mellitus. Med Hypotheses 1995; 45: 486–90.

Koval ED, Shaner C, Zhang P, du Maine X, Fischer K, Tay J, et al. Method for widespread microRNA-155 inhibition prolongs survival in ALS-model mice. Hum Mol Genet 2013; 22: 4127–35.

Lawrie CH, Gal S, Dunlop HM, Pushkaran B, Liggins AP, Pulford K, et al. Detection of elevated levels of tumour-associated microRNAs in serum of patients with diffuse large B-cell lymphoma. Br J Haematol 2008; 141: 672–5.

Lehmann SM, Kruger C, Park B, Derkow K, Rosenberger K, Baumgart J, et al. An unconventional role for miRNA: let-7 activates Toll-like receptor 7 and causes neurodegeneration. Nat Neurosci 2012; 15: 827–35.

Liddelow SA, Guttenplan KA, Clarke LE, Bennett FC, Bohlen CJ, Schirmer L, et al. Neurotoxic reactive astrocytes are induced by activated microglia. Nature 2017; 541: 481–7.

Lim LP, Lau NC, Garrett-Engele P, Grimson A, Schelter JM, Castle J, et al. Microarray analysis shows that some microRNAs downregulate large numbers of target mRNAs. Nature 2005; 433: 769–73.

Madji Hounoum B, Mavel S, Coque E, Patin F, Vourc'h P, Marouillat S, et al. Wildtype motoneurons, ALS-Linked SOD1 mutation and glutamate profoundly modify astrocyte metabolism and lactate shuttling. Glia 2017; 65: 592–605.

Mittelbrunn M, Gutierrez-Vazquez C, Villarroya-Beltri C, Gonzalez S, Sanchez-Cabo F, Gonzalez MA, et al. Unidirectional transfer of microRNA-loaded exosomes from T cells to antigen-presenting cells. Nat Commun 2011; 2: 282.

Mullick A, Xu Y, Warren R, Koutroumanis M, Guilbault C, Broussau S, et al. The cumate gene-switch: a system for regulated expression in mammalian cells. BMC Biotechnol 2006; 6: 43.

Prakash TP, Graham MJ, Yu JH, Carty R, Low A, Chappell A, et al. Targeted delivery of antisense oligonucleotides to hepatocytes using triantennary N-acetyl galactosamine improves potency 10-fold in mice. Nucleic Acids Res 2014; 42: 8796–807.

Ravits J, Laurie P, Fan YX, Moore DH. Implications of ALS focality—rostral-caudal distribution of lower motor neuron loss postmortem. Neurology 2007; 68: 1576–82.

Rothstein JD, Van Kammen M, Levey AI, Martin LJ, Kuncl RW. Selective loss of glial glutamate transporter GLT-1 in amyotrophic lateral sclerosis. Ann Neurol 1995; 38: 73–84.

Saetrom P, Heale BS, Snove O, Aagaard L, Alluin J, Rossi JJ. Distance constraints between microRNA target sites dictate efficacy and cooperativity. Nucleic Acids Res 2007; 35: 2333–42.

Shobha K, Vijayalakshmi K, Alladi PA, Nalini A, Sathyaprabha TN, Raju TR. Altered in-vitro and in-vivo expression of glial glutamate transporter-1 following exposure to cerebrospinal fluid of amyotrophic lateral sclerosis patients. J Neurol Sci 2007; 254: 9–16.

Simeoli R, Montague K, Jones HR, Castaldi L, Chambers D, Kelleher JH, et al. Exosomal cargo including microRNA regulates sensory neuron to macrophage communication after nerve trauma. Nat Commun 2017; 8: 1778.

Sun SY, Sun Y, Ling SC, Ferraiuolo L, McAlonis-Downes M, Zou YY, et al. Translational profiling identifies a cascade of damage initiated in motor neurons and spreading to glia in mutant SOD1-mediated ALS. Proc Natl Acad Sci USA 2015; 112: E6993–7002.

Thiebes KP, Nam H, Cambronne XA, Shen R, Glasgow SM, Cho HH, et al. miR-218 is essential to establish motor neuron fate as a downstream effector of Isl1-Lhx3. Nat Commun 2015; 6: 7718.

Turchinovich A, Weiz L, Langheinz A, Burwinkel B. Characterization of extracellular circulating microRNA. Nucleic Acids Res 2011; 39: 7223–33.

Unger T, Bette S, Zhang J, Theis M, Engele J. Connexin-deficiency affects expression levels of glial glutamate transporters within the cerebrum. Neurosci Lett 2012; 506: 12–16.

Valadi H, Ekstrom K, Bossios A, Sjostrand M, Lee JJ, Lotvall JO. Exosome-mediated transfer of mRNAs and microRNAs is a novel mechanism of genetic exchange between cells. Nat Cell Biol 2007; 9: 654–9.

Van Damme P, Bogaert E, Dewil M, Hersmus N, Kiraly D, Scheveneels W, et al. Astrocytes regulate GluR2 expression in motor neurons and their vulnerability to excitotoxicity. Proc Natl Acad Sci USA 2007; 104: 14825–30.

Wang K, Zhang S, Weber J, Baxter D, Galas DJ. Export of microRNAs and microRNA-protective protein by mammalian cells. Nucleic Acids Res 2010; 38: 7248–59.

Yamanaka K, Boillee S, Roberts EA, Garcia ML, McAlonis-Downes M, Mikse OR, et al. Mutant SOD1 in cell types other than motor neurons and oligodendrocytes accelerates onset of disease in ALS mice. Proc Natl Acad Sci USA 2008a; 105: 7594–9.

Yamanaka K, Chun SJ, Boillee S, Fujimori-Tonou N, Yamashita H, Gutmann DH, et al. Astrocytes as determinants of disease progression in inherited amyotrophic lateral sclerosis. Nat Neurosci 2008b; 11: 251–3.

Zhang B, Gaiteri C, Bodea LG, Wang Z, McElwee J, Podtelezhnikov AA, et al. Integrated systems approach identifies genetic nodes and networks in late-onset Alzheimer's disease. Cell 2013; 153: 707–20.

Zhang Y, Chen KN, Sloan SA, Bennett ML, Scholze AR, O'Keeffe S, et al. An RNA-sequencing transcriptome and splicing database of glia, neurons, and vascular cells of the cerebral cortex. J Neurosci 2014; 34: 11929–47.

Zhang Y, Jia Y, Zheng R, Guo Y, Wang Y, Guo H, et al. Plasma microRNA-122 as a biomarker for viral-, alcohol-, and chemical-related hepatic diseases. Clin Chem 2010; 56: 1830–8.